

¹¹D. J. Kim and B. B. Schwartz, Phys. Rev. Letters **21**, 1744 (1968).

¹²M. F. Sykes and J. W. Essam, Phys. Rev. **133**, A310 (1964).

¹³J. W. Cable, E. O. Wollan, and H. R. Child, Phys. Rev. Letters **22**, 1256 (1969); C. G. Robbins, H. Claus,

and P. A. Beck, *ibid.* **22**, 1307 (1969).

¹⁴H. C. Van Elst, B. Lubach, and G. J. VandenBerg, Physica **28**, 1297 (1962). See also A. Hahn and E. P. Wohlfarth [Helv. Phys. Acta **41**, 857 (1968)] for evidence of superparamagnetism in Ni-Rh.

¹⁵R. B. Griffiths, Phys. Rev. Letters **23**, 17 (1969).

PHYSICAL REVIEW B

VOLUME 2, NUMBER 3

1 AUGUST 1970

Study of Far-Infrared Excitations in Metamagnetic $\text{FeCl}_2 \cdot 2\text{H}_2\text{O}^\dagger$

K. A. Hay*

and

J. B. Torrance, Jr.‡

Division of Engineering and Applied Physics, Harvard University, Cambridge, Massachusetts

(Received 2 February 1970)

The spin-wave spectra in the antiferromagnetic, ferrimagnetic, and ferromagnetic phases of $\text{FeCl}_2 \cdot 2\text{H}_2\text{O}$ have been examined at 2 and 6 °K. These spectra are well described by a spin-wave calculation; it is shown that $g_{11} = 2.23 \pm 0.02$, $S = 2$, and that the exchange interactions are isotropic. The (large) longitudinal anisotropy is included in the Hamiltonian as a single-ion anisotropy ($D = +9.58 \pm 0.05 \text{ cm}^{-1}$), which is shown to make an anomalously large contribution to the spin-wave energies. These results are discussed and interpreted from the point of view of crystal-field theory. In all three metamagnetic phases, the magnetic resonance modes are observed to interact with a field-independent excitation with energy 31.5 cm^{-1} , which is presumably an optical phonon. The measured value of the metamagnetic transition field $H_{c2} = 45.0 \pm 0.5 \text{ kOe}$ compares quite well with Narath's value of 45.6 kOe, but our value of $H_{c1} = 35.0 \pm 0.5 \text{ kOe}$ is in poor agreement with Narath's 39.2 kOe. Near H_{c1} (the antiferromagnetic-to-ferrimagnetic transition field), the far-infrared spectrum appears to indicate that both antiferromagnetic and ferrimagnetic "domains" coexist over a certain range of field. The temperature dependence and hysteresis of these domains are also described and compared with Tinkham's microscopic description of these transitions.

I. INTRODUCTION

Ferrous chloride dihydrate is one of a family of crystals which exhibit strong exchange interactions along one crystallographic axis and weak interactions perpendicular to this axis. The initial magnetic measurements on $\text{FeCl}_2 \cdot 2\text{H}_2\text{O}$ (or more briefly FC2) were performed by Narath¹ and are reviewed in this section. In Sec. II our experimental techniques and procedures are described. The results of the far-infrared measurements in all three metamagnetic regions are shown in Sec. III to determine both the magnitude and anisotropy of some of the exchange interactions. These results are interpreted in terms of crystal-field theory (Sec. IV) and compared to the results of Johnson² and of Inomata and Oguchi³ (which are in disagreement). In Sec. V the observed coexistence of antiferromagnetic and ferrimagnetic resonance modes at the same field is described. The results of this work are summarized and discussed in Sec. VI

and compared to the results on $\text{CoCl}_2 \cdot 2\text{H}_2\text{O}$ (CC2).⁴

One of the most prominent features of the data is a phonon which is observed to interact with the magnon states. This interaction is only briefly described in this paper, as it is discussed in more detail elsewhere,⁵ together with the observation of a similar level in CC2.

Ferrous chloride dihydrate (FC2) crystallizes in linear chains of $-\text{FeCl}_2-$ which run along the c axis.⁶ The exchange interaction J_0 between Fe^{2+} spins within the same chain is ferromagnetic and much stronger than the antiferromagnetic interactions between chains. The chemical bonding within a chain is similarly stronger than the weak forces between chains; hence, the crystals cleave easily parallel to the c -axis. The crystal symmetry is monoclinic with a twofold axis (b) and a mirror plane (ac). Although the unit cell contains two formula units, these are equivalent. Narath¹ points out that magnetic canting effects are not expected because the midpoints between

nearest (intrachain) and next-nearest (interchain) ion pairs are centers of inversion.

Narath has studied the magnetic properties of FC2 and found a transition at 23 °K to the two sublattice antiferromagnetic (AF) state shown in Fig. 1(a). This figure represents a typical cross section through the chains of spins, which are coming out of the plane of the figure. The spins within a chain are ferromagnetically aligned due to the strong intrachain interaction J_0 . The weaker antiferromagnetic interactions J_1 and J_2 are shown in Fig. 1. (J_3 is probably very small and we neglect it.) Measurements of the low-temperature magnetization in large external fields reveal metamagnetic transitions to a three sublattice ferrimagnetic (Fi) state [Fig. 1(b)] at $H_{C1} = 39.2$ kOe and to a ferromagnetic (Fo) state [Fig. 1(c)] at $H_{C2} = 45.6$ kOe.¹ The measured magnetic moments in these states are $\mu_{Fi} = (1.4 \pm 0.1)\mu_B$ and $\mu_{Fo} = (4.25 \pm 0.05)\mu_B$ per Fe^{2+} ion. Narath¹ also studied the proton NMR and the static susceptibility; he found that the axis of magnetization (α) lies in the ac plane, as shown in Fig. 2. (It should be noted that Fig. 1 shows only the *component* of the spin in the ab plane.) The other principal axes of the magnetic tensor are determined when it is realized that the crystal symmetry demands that one must coincide with the twofold b axis (γ). The other, β , must then be normal to α and γ (b), in the ac plane (Fig. 2). When the paramagnetic susceptibility data were fitted to a simple Curie-Weiss relation,⁷ it was found¹ that $g_\alpha^2 S(S+1) = 34.6$, $g_{\beta,\gamma}^2 S(S+1) = 21.7$, with Weiss constants $\Delta_\alpha = +12$ °K and $\Delta_\beta = \Delta_\gamma = +5$ °K. Note that the magnetic anisotropy appeared uniaxial about α . These measurements do not determine the value S of the spin of the ground

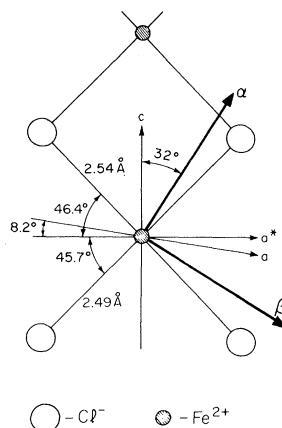


FIG. 2. Axis of magnetization of $\text{FeCl}_2 \cdot 2\text{H}_2\text{O}$ is the direction α , lying in the ac plane. The other principal magnetic axes are β and γ , which coincide with the crystallographic b axis and are normal to the plane of the figure (after Narath, see Ref. 1).

state, but for $S = 2$ we obtain $g_\alpha = 2.4$ and $g_\beta = g_\gamma = 1.9$.

II. EXPERIMENTAL

Crystals of $\text{FeCl}_2 \cdot 2\text{H}_2\text{O}$ (FC2) were grown by slowly evaporating a saturated ferrous chloride solution in a carefully regulated (± 0.05 °C) oven for 3–4 weeks. Initially, the crystals were grown at 75 °C as prescribed by Narath¹ and the results were largely unsatisfactory: The crystals were small and often had holes along their length, as Narath found. When a higher temperature of 85 °C was tried, the results were generally more satisfactory, with single crystals up to $1 \times 1 \times 8$ cm in size. These crystals were nearly transparent, with a lime green coloration. Neither precipitation of iron oxide nor crystal twinning have appeared to be serious problems.

Crystal orientation was determined by three methods: (i) by Laue back-reflection x-ray tech-

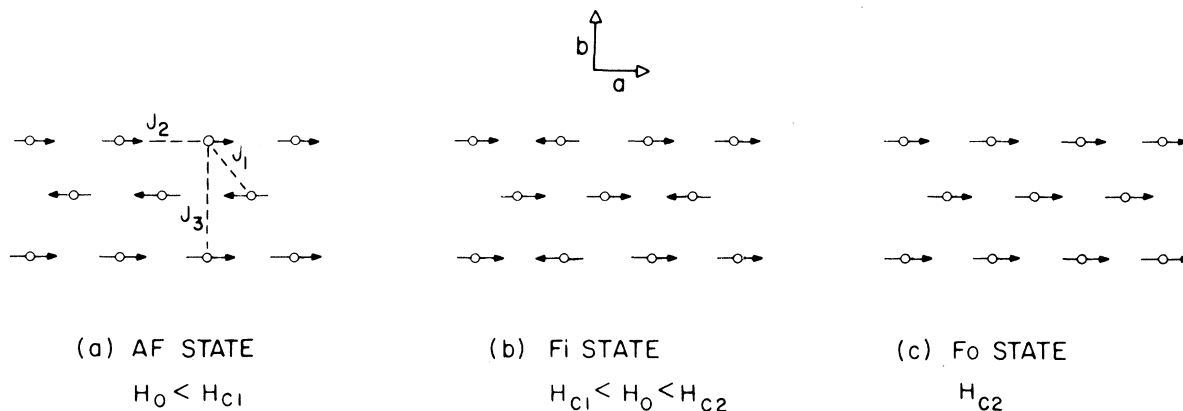


FIG. 1. (a) Antiferromagnetic (AF), (b) ferrimagnetic (Fi), and (c) ferromagnetic (Fo) spin structures of $\text{FeCl}_2 \cdot 2\text{H}_2\text{O}$ for the external field H_0 along the α axis. This figure shows a cross section through the chains of ferromagnetically aligned spins. Since the spin directions lie along α (Fig. 2), the arrows indicate only the *projection* of the moments on the ab plane.

niques; (ii) by allowing the crystal to orient in a field⁸ of a few kOe (at room temperature the α axis aligns parallel to the external field); and (iii) from the morphology. The crystals grow as slender prismatic needles, defining the c axis. The side faces of the needles are (110) and ($\bar{1}10$) planes, which indicate the b axis, but not the a axis since the crystal is monoclinic, i. e., there is still an uncertainty in the direction of the positive c axis. This ambiguity can be resolved if the end faces can be seen, since these faces are ($\bar{2}01$) planes.

Samples in the form of thin plates were made by cleaving the crystals to expose the ac plane. The α axis can then be aligned along the external field in order to make the measurements described here. In this geometry, demagnetization effects are minimized since the α axis is in the plane of the sample. Although three different samples were used, most of the data presented in this paper were taken with a crystal approximately 13 mm long in the direction of the external magnetic field and 1.2 mm thick. If this geometry is approximated to an ellipsoid, demagnetizing fields of 260 Oe in the ferromagnetic region and 85 Oe in the ferrimagnetic state are expected.⁹

Experimentally, the object was to measure the far-infrared absorption spectrum of FC2. Some preliminary experiments were carried out at zero magnetic field using a Michelson interferometer. It was found much more convenient, however, to use a far-infrared grating monochromator¹⁰ to make the many measurements necessary to determine the complete spectrum as a function of applied field. The use of a monochromator also made possible experiments in which the magnetic field was swept at constant photon energy. (This was useful in examining the hysteretic behavior of the spectrum near H_{C1} .) A data processing system^{11,12} which integrated the far-infrared detector response over increments of grating angle and transferred the data to computer cards was extremely useful in making the spectra accessible for careful and accurate study. A computer was used to compensate for variations in the background response for different energies (by a ratio technique) and to plot the spectra as functions of energy. Since the data were stored in numerical form, it was possible to choose an optimum quartic smoothing function. This scheme gave a significant improvement over traditional RC-type data averaging.

The radiation from the monochromator was directed via $\frac{1}{2}$ -in. brass light pipe into a cryostat and through the sample to a gallium-doped germanium bolometer, which was cooled to 1.1 °K. The sample was glued to a wedged quartz substrate with G. E. -7031 varnish to provide good thermal contact and then mounted in the center of a super-

conducting solenoid.¹³ The sample temperature could be altered between 2 and 30 °K by a heater attached to the quartz substrate. For measurements above 10 °K, it was necessary to reduce the effectiveness of the thermal link between the substrate and the 1.1 °K helium bath by inserting a section of stainless steel rod. The far-infrared radiation was polarized using polarizers made with gold lines deposited on Mylar.¹⁴

III. FAR-INFRARED SPECTRA

A magnetic-field-dependent spectrum has been observed in $\text{FeCl}_2 \cdot 2\text{H}_2\text{O}$ (FC2) in the energy range 28–37 cm^{-1} . This spectrum was studied in magnetic fields of 0–55 kOe with the field aligned parallel to α to within 1°. Some typical transmission spectra are shown in Fig. 3. The observed resonance frequencies are plotted in Fig. 4 against the applied magnetic field. Far-infrared measurements on $\text{CoCl}_2 \cdot 2\text{H}_2\text{O}$ (CC2)^{4, 10, 15} indicate that the spin-wave resonances absorb the magnetic component of the radiation oscillating in the plane perpendicular to the axis of magnetization. The resonances observed in FC2 are consistent with this type of magnetic dipole absorption. Strong Reststrahl absorption is observed above 140 cm^{-1} , making far-infrared measurements above this energy impossible. A description of the complex nature of the spectrum near H_{C1} is postponed until Sec. V.

The most striking features of the spectrum (Fig. 4) are the discontinuities at the metamagnetic transition fields, H_{C1} and H_{C2} , and the observation of an extra, unexpected excitation. In the antiferro-

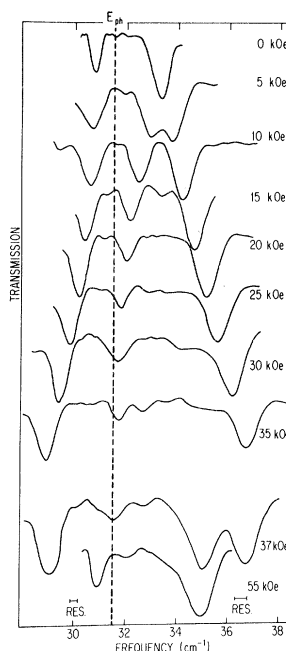


FIG. 3. Experimental transmission spectra for $\text{FeCl}_2 \cdot 2\text{H}_2\text{O}$ at 2 °K, showing evidence of the magnon-phonon interactions in the antiferromagnetic state (< 35 kOe). The dashed line is the unperturbed phonon energy. The spectrum at 37 kOe was taken as the field was being increased from the antiferromagnetic phase, while the spectrum at 55 kOe was taken in the ferromagnetic phase.

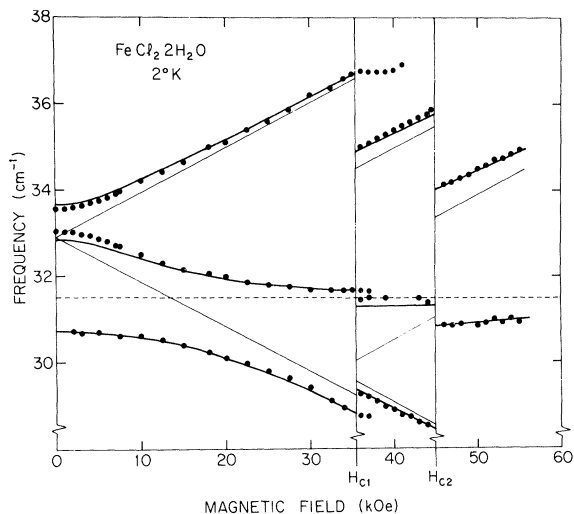


FIG. 4. The far-infrared spectrum of $\text{FeCl}_2 \cdot 2\text{H}_2\text{O}$. The experimentally observed resonances (solid points), the theoretical, unperturbed spin-wave energies (narrow lines), and the phonon (dashed line) are all plotted against the applied magnetic field. The heavy lines are the result of including a phenomenological magnon-phonon interaction. Absorption due to the phonon in the ferrimagnetic phase is weak.

magnetic state, for example, two magnetic resonances would be expected, corresponding to the two sublattices; however, three absorption lines are observed. Furthermore, this unexpected, extra excitation appears to interact with the two magnetic modes. It is possible to qualitatively understand the observed spectrum if one assumes that the two antiferromagnetic resonance (AFMR) excitations interact with a third field-independent excitation $|\text{ph}\rangle$ whose energy E_{ph} is shown by the dashed line in Figs. 3 and 4. In order to describe this interaction quantitatively, we assume that a phenomenological coupling energy exists between $|\text{ph}\rangle$ and the AFMR modes (which are calculated below and shown by the narrow lines in Fig. 4). Characterizing this coupling by an off-diagonal matrix element A_{AF} between the states, the perturbed energies are calculated. The heavy lines in Fig. 4 represent the results for $A_{\text{AF}} = 0.94 \text{ cm}^{-1}$ and $E_{\text{ph}} = 31.5 \text{ cm}^{-1}$. The calculated curves agree with the data to within a fraction of the measured linewidth ($\approx 0.6 \text{ cm}^{-1}$). In the ferromagnetic region, the interaction between $|\text{ph}\rangle$ and the expected ferromagnetic resonance mode causes the levels to repel. This effect is described phenomenologically as above, using the same value of E_{ph} . Unfortunately, this analysis is difficult to carry over to the ferrimagnetic region, since the absorption associated with $|\text{ph}\rangle$ is much weaker than in the other two re-

gions, precluding an accurate fit of the data.⁵

Note in Fig. 3 that the intensity of absorption of $|\text{ph}\rangle$ is strongest where the interaction with the magnons is largest ($\sim 10 \text{ kOe}$) and weakest near H_{C1} where the interaction is weak. This fact suggests that $|\text{ph}\rangle$ is only infrared active because of the admixture of magnons. The fact that the unperturbed energy of this extra excitation is field independent, even through H_{C1} and H_{C2} where the magnetic structure changes drastically, strongly suggests that $|\text{ph}\rangle$ is a nonmagnetic excitation. In Ref. 5 it is argued that it is, in fact, a low-lying $k=0$ optical phonon. A similar excitation is also observed in $\text{CoCl}_2 \cdot 2\text{H}_2\text{O}$ and is described by the same analysis.^{4,5} Recently, Allen and Guggenheim¹⁶ have observed an optical phonon in CoF_2 which appears coupled to the magnetic excitations in that material.

A. Theory

The spin-wave energies (the narrow lines in Fig. 4) are calculated in a straightforward manner using the traditional linear spin-wave theory.¹⁷ The magnetic symmetry is observed to be (accidentally) uniaxial¹ (Sec. IV) and the longitudinal anisotropy (along α) is described by the parameter D (single-ion anisotropy). If we include the possibility of an anisotropic exchange interaction, the appropriate spin Hamiltonian, for effective spin S , is given by

$$\mathcal{H} = - \sum_i g_{\parallel} \mu_B H_0 S_i^z - D \sum_i [(S_i^z)^2 - \frac{1}{3} S(S+1)] - \sum_{i,\delta} J_{\delta}^1 \tilde{S}_i \cdot \tilde{S}_{i+\delta} - \sum_{i,\delta} J_{\delta}^A S_i^z S_{i+\delta}^z, \quad (1)$$

where the external magnetic field H_0 is parallel to $z(\alpha)$, the axis of magnetization. The exchange parameters J_{δ}^1 and J_{δ}^A couple a spin S_i at site i to a spin $S_{i+\delta}$ and are defined as

$$J_{\delta}^1 \equiv J_{\delta}^{xx} = J_{\delta}^{yy}, \quad J_{\delta}^A \equiv J_{\delta}^{zz} - J_{\delta}^{xx}. \quad (2)$$

This way of decomposing the exchange interaction separates the isotropic or "Heisenberg" part J_{δ}^1 from the longitudinally anisotropic part J_{δ}^A (which is often described¹⁷ by an anisotropy field H_A); this notation is consistent with that used in the calculations for CC2.⁴ The exchange paths for FC2 are shown in Fig. 1, with the exception of J_0 , which is the exchange interaction between spins neighboring along a chain. J_0 is known to be strong and ferromagnetic (hence positive), while J_1 and J_2 are antiferromagnetic¹ (negative). J_3 is probably ferromagnetic, but very small as in CC2. In these experiments its effect is indistinguishable from that of J_0 and for this reason it is neglected.

Using the Hamiltonian (1) and the spin structures (Fig. 1) the spin-wave energies at $k=0$ may be cal-

culated.¹⁰ The results are summarized below:

$$E_{AF}^+ = E_0 + \frac{1}{3}(2E_{C1}^A + E_{C2}^A) + \frac{1}{3}(E_{C1}^L + 2E_{C2}^L) - \delta_{AF} \pm g_{\parallel} \mu_B H_0, \quad (3)$$

$$E_{F1}^+ = E_0 + \frac{1}{2}E_{C2}^L - \delta_{F1} + g_{\parallel} \mu_B H_0, \quad (4)$$

$$E_{F1}^- = E_0 + E_{C2}^A + E_{C2}^L - \delta_{F1} - g_{\parallel} \mu_B H_0, \quad (5)$$

$$E_{F1}^* = E_0 - \frac{1}{2}E_{C2}^L + g_{\parallel} \mu_B H_0, \quad (6)$$

$$E_{F0} = E_0 - E_{C2}^A + g_{\parallel} \mu_B H_0. \quad (7)$$

In these results we have used several parameters which are defined as follows:

$$E_0 \equiv D(2S - 1) + 2p_0 J_0^A S, \quad (8)$$

$$E_{C1}^L \equiv 2S(p_1 | J_1^L | - 2p_2 | J_2^L |), \quad (9)$$

$$E_{C2}^L \equiv 2S(p_1 | J_1^L | + p_2 | J_2^L |), \quad (10)$$

$$\delta_{AF} = (E_{C1}^L + 2E_{C2}^L)^2 / 18 E_0, \quad (11)$$

$$\delta_{F1} = (E_{C2}^L)^2 / 4 E_0,$$

where p_6 is the number of neighbors coupled by J_6 and with definitions for E_{C1}^A and E_{C2}^A analogous to (9) and (10). It should be noted that the expressions for δ_{AF} and δ_{F1} are valid only in the case of strong longitudinal anisotropy. Two additional relations¹⁸ are useful to relate the transition fields H_{C1} and H_{C2} to E_{C1} and E_{C2} :

$$g_{\parallel} \mu_B H_{C1} = 2S(p_1 | J_1^{zz} | - 2p_2 | J_2^{zz} |) = E_{C1}^L + E_{C1}^A, \quad (12)$$

$$g_{\parallel} \mu_B H_{C2} = 2S(p_1 | J_1^{zz} | + p_2 | J_2^{zz} |) = E_{C2}^L + E_{C2}^A. \quad (13)$$

Note that each of the spin-wave energies has a term E_0 [Eq. (8)], i. e., both D and the exchange anisotropy in J_0 contribute to the excitation energy of each mode (similar to an anisotropy field). This part of the energy will be seen to be very large, because of the large longitudinal anisotropy of FC2. Note also the form of the contribution $D(2S - 1)$ of the D term, which vanishes for $S = \frac{1}{2}$, as it should.

B. Results

The spin-wave energies are uniquely determined by five independent parameters, but there are six available. In order to reduce this number, we make the assumption that $J_1^A/J_1^L = J_2^A/J_2^L$, i. e., that the anisotropy in J_1 is the same as that in J_2 . The experimental data may now be fitted using the spin-wave energies (3)–(7) and the phenomenological magnon-phonon coupling.⁵ The best fit obtained is shown by the heavy lines in Fig. 4. The following five parameters were used in that fit:

$$g_{\parallel} = 2.23 \pm 0.02,$$

$$E_0 = 28.75 \pm 0.15 \text{ cm}^{-1},$$

$$H_{C1} = 35.0 \pm 0.5 \text{ kOe},$$

$$H_{C2} = 45.0 \pm 0.5 \text{ kOe},$$

$$J_1^A/J_1^L = J_2^A/J_2^L < 0.03.$$

Measurements of the spin-wave energies in all three metamagnetic phases have enabled us to determine not only the magnitude of J_1 and J_2 , but also their anisotropy. The observed anisotropy is the same order of magnitude as both the experimental error and the expected dipole-dipole contribution. For this reason, we conclude that the exchange interactions J_1 and J_2 are *isotropic* and have magnitudes [from (12) and (13)] given by

$$J_1 = J_1^L - 0.27 \text{ cm}^{-1}, \quad J_2 = J_2^L = -0.044 \text{ cm}^{-1}.$$

Since these two exchange interactions are isotropic, it is not unreasonable to assume that J_0 is also isotropic. In that case the strong longitudinal magnetic anisotropy is completely contained in the D -term, with $D = +9.58 \pm 0.05 \text{ cm}^{-1}$. [A small anisotropy in (large) J_0 would, however, decrease this value significantly.] It has not been found necessary to include any *transverse* magnetic anisotropy (i. e., rhombic distortion), although the interaction of the phonon at zero field would tend to mask a small rhombic splitting of the spin-wave states at zero field. In the susceptibility data, Narath¹ also found negligible transverse anisotropy and one must conclude that, although it is allowed by the symmetry of the Fe^{2+} site, it is small.

Narath¹ has measured the saturation magnetization in the ferromagnetic state, which gives $g_{\parallel} S = 4.25 \pm 0.05$ for the ground state. This value may be somewhat low due to imperfect sample alignment, but if we use the g value found from the far-infrared experiments ($g_{\parallel} = 2.23$), we find that $S \approx 2$, which is the free ion value. This is in contradiction to the work of Inomata and Oguchi,³ who predicted a value of $S = 1$, but it is in agreement with Johnson,² who used $S = 2$ to analyze his Mössbauer data (see Sec. IV).

In the Fi state, three magnetic modes are predicted and shown in Fig. 4. These correspond to the three sublattices, but only two of the modes are observed (Fig. 3). The third mode E_{Fi}^* (6) is the “silent” mode and is not infrared active¹⁹; it corresponds to the two equivalent “up” sublattices precessing in such a way that there is no oscillating net moment in the xy plane to which the radiation can couple. It should also be noted that the fit of the data near zero field is not as good as at higher fields. The experimental error is larger near zero field, since there the linewidth ($\approx 0.6 \text{ cm}^{-1}$) becomes comparable to the line splitting, and the resonance frequencies are obtained only after a careful examination of the broadened linewidths.

The temperature dependence of the spectrum has not been studied in detail, but the general variation

of the zero-field resonances with temperature is shown in Fig. 5. Although the linewidth broadens as the temperature is increased, there is little change in the energy of the resonances until very near the Néel temperature, as expected due to the strong anisotropy of FC2.²⁰ Near this temperature 23 °K a very broad absorption band appears at lower energies which is also observed at temperatures above 23 °K.

IV. CRYSTAL-FIELD THEORY

The ground state of a free Fe^{2+} ion is 5D . This level is split by the octahedral component of the crystal field into an orbital triplet ($^5T_{2g}$), which lies $\Delta \approx 10^4 \text{ cm}^{-1}$ below an orbital doublet (5E_g). (We have confirmed this splitting by optical measurements.) The energies of the $^5T_{2g}$ wave functions $|xy\rangle$, $|xz\rangle$, and $|yz\rangle$ are then split by the rhombic part of the crystal field. Since the complete effects of this distortion, the spin-orbit interaction, and covalency are extremely difficult to predict, we must regard the $^5T_{2g}$ splittings as fitting parameters. If we assume that a single one of the $^5T_{2g}$ states lies lowest and is separated from the others by an energy large compared to the spin-orbit coupling constant $|\lambda|$, the perturbation procedure of Abragam and Pryce²¹ may be applied for a crude description of the lowest-lying states. For $\text{FeCl}_2 \cdot 2\text{H}_2\text{O}$ this assumption is reasonable since the g values are approximately 2. (If the splitting were comparable to $|\lambda|$, large departures from $g \sim 2$ would be expected.)

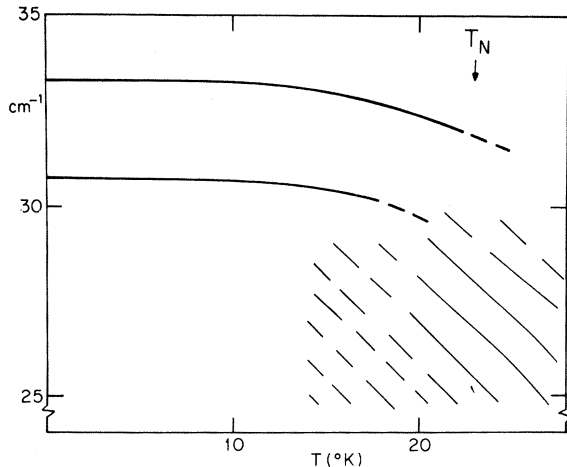


FIG. 5. Temperature dependence of the absorption at zero magnetic field. At 12 °K the absorption has become very intense and broad ($\sim 2.5 \text{ cm}^{-1}$ wide for the upper mode). At higher temperatures, both absorptions become progressively weaker, giving way to a general absorption at lower energies, shown shaded.

The lowest-lying states of the Fe^{2+} ion in a rhombic crystal field with principal axes x, y, z may be described by the following spin Hamiltonian:

$$\mathcal{H}_{\text{Fe}^{2+}} = -D[S_z^2 - \frac{1}{3}S(S+1)] - E[S_x^2 - S_y^2], \quad (14)$$

where the longitudinal anisotropy along z and the transverse (rhombic) anisotropy in the xy plane are described by the parameters D and E , respectively. From Sec. III we also have $S = 2$. The $^5T_{2g}$ states are split by the rhombic crystal field such that $E_{xz} = 0$, $E_{xy} = \Delta_x$, and $E_{yz} = \Delta_y$, assuming that $|xz\rangle$ lies lowest. If $\Delta_x, \Delta_y \gg |\lambda|$, the following relations²¹ hold for the ground-state g values and the parameters D and E of (14)

$$\begin{aligned} g_x &= 2 - 2\lambda/\Delta_x, \quad g_y = 2 - 8\lambda/\Delta, \quad g_z = 2 - 2\lambda/\Delta_y, \\ D &= \lambda^2(1/\Delta_x - 1/2\Delta_x - 2/\Delta), \quad E = \lambda^2(1/2\Delta_x - 2/\Delta), \end{aligned} \quad (15)$$

where λ is the spin-orbit coupling constant and $\Delta \approx 10^4 \text{ cm}^{-1}$ is the $^5T_{2g} - ^5E_g$ splitting. $|\lambda|$ is smaller than the free ion value ($\lambda_0 = -104 \text{ cm}^{-1}$) because of covalency effects.^{21,22} We must now assume that the principal axes of the crystal field (z, x, y) correspond to the principal axes of the magnetization (α, β, γ in Fig. 2).

Measurements of the paramagnetic susceptibility¹ indicate that α (Fig. 2) is the axis of magnetization and that the magnetic symmetry is approximately *uniaxial* about that axis, i. e., $E = 0$. The far-infrared measurements (Sec. III) are consistent with these results and, in addition, reveal that $D = +9.58 \text{ cm}^{-1}$, $g_\alpha = 2.23$, and $S = 2$ for the ground state. It can be seen from (15) that the magnetic anisotropy would appear uniaxial if $\Delta = 4\Delta_x$, i. e., if there were a certain relationship between the rhombic and cubic components of the crystal field. Since the crystal field is certainly *not* uniaxial about α , this magnetic symmetry must be *accidental*. With $\Delta = 4\Delta_x = 4\Delta_y$ we find that

$$\begin{aligned} g_{\parallel} &= g_\alpha = 2 - 2\lambda/\Delta_\alpha, \\ g_{\perp} &= g_\beta = g_\gamma = 2 - 8\lambda/\Delta, \\ D &= \lambda^2(1/\Delta_\alpha - 4/\Delta). \end{aligned} \quad (16)$$

For $\Delta = 10^4 \text{ cm}^{-1}$, $\lambda = 95 \text{ cm}^{-1}$, and choosing $\Delta_\alpha = 720 \text{ cm}^{-1}$, we obtain $D = +8.8 \text{ cm}^{-1}$, $g_{\parallel} = 2.26$, and $g_{\perp} = 2.08$. These values are in reasonable agreement with the observed single-ion anisotropy parameter $D = +9.58 \text{ cm}^{-1}$ and $g_{\parallel} = 2.23$, considering the crudeness of the theory which leads to (15).

In this analysis we have assumed that $|xz\rangle$ was the lowest $^5T_{2g}$ level. If we had chosen $|xy\rangle$ instead, we would have obtained $g_{\parallel} = 2 - 8\lambda/\Delta = 2.06$ and $D < 0$; both results are in disagreement with experiment. If $|yz\rangle$ were chosen as the ground orbital, the values of g_{\parallel} and D would be the same

as for $|xz\rangle$. We would imagine that $|xz\rangle$ would be lowest, however, since its lobes lie in the xz (ac) plane of the crystal, contributing to the strong bonding between the Fe^{2+} and the neighboring Cl^- ions. This supposition is verified by the Mössbauer work on $\text{FeCl}_2 \cdot 2\text{H}_2\text{O}$ of Johnson,² who finds that the ground state is predominantly $|xz\rangle$. Johnson carried out a similar crystal-field analysis, using a rhombic crystal field, and also finds that $S = 2$. Inomata and Oguchi,³ on the other hand, used a different approach: they obtained uniaxial magnetic symmetry by assuming a uniaxial crystal field along a and concluded that $S = 1$ for the ground state, in disagreement with experiment.

The values of g_{\parallel} and D which we have measured in $\text{FeCl}_2 \cdot 2\text{H}_2\text{O}$ are remarkably similar to those in FeF_2 , where $S = 2$, $g_{\parallel} = 2.25$, and $D = +9 \pm 2 \text{ cm}^{-1}$.²³ As a possible indication of the magnitude of E , Tinkham²⁴ estimates $E \sim 0.7 \text{ cm}^{-1}$ for Fe^{2+} in ZnF_2 .

V. HYSTERETIC BEHAVIOR OF LINES NEAR H_{C1}

An inspection of Figs. 3 and 4 shows that, in addition to the predicted spin-wave modes and the phonon,⁵ there apparently exist antiferromagnetic (AF) resonance modes above H_{C1} , i. e., in the ferrimagnetic state. This absorption is assumed to be due to antiferromagnetically ordered "domains" which persist above the transition field. Similar effects have also been observed in $\text{CoCl}_2 \cdot 2\text{H}_2\text{O}$ ⁴ and $\text{CoBr}_2 \cdot 2\text{H}_2\text{O}$,²⁵ but in FC2 we have carried out an examination of their hysteresis and temperature dependence. The relative absorption intensity of this AF line may be used to give a measure of the amount of AF "domains" above H_{C1} , from which we can infer the magnetization M . The magnetization-versus-field curves predicted on this basis are shown in Fig. 6 for 2 and 6 °K, along with the observed 4.2 °K magnetization.¹ (There is no mention of hysteresis in the magnetization experiments.)

The most likely source of such hysteresis is demagnetization effects. In FeCl_2 , for example, AF and Fo resonance modes were observed²⁶ to coexist at the AF-Fo metamagnetic transition field. In that case, however, the sample-field geometry gave rise to large demagnetizing fields, which stabilized the AF and Fo domains. In our experiments the sample-field geometry is expected to give rise to demagnetization fields less than 85 Oe, while the domains appear to persist over a 6000-Oe range. It is possible that the noncubic part of the demagnetization field might play an important role in monoclinic FC2, but demagnetization effects alone cannot account for the observed hysteresis for two *additional* reasons: (i) Such a demagnetization theory would predict persisting domains and hysteresis at H_{C2} , where neither are observed.

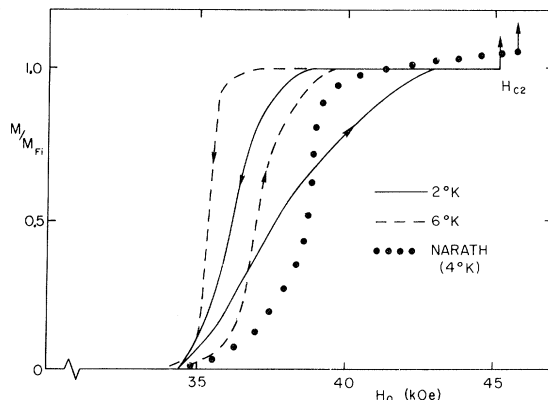


FIG. 6. Hysteresis of the magnetization M in the ferrimagnetic phase. $M_{F1} = 1.4 \mu_B/\text{Fe}^{2+}$ ion. Our 2 and 6 °K magnetization data were *inferred* from the relative intensity of the AF and Fi absorption lines. (The error on these ratios is $\sim 20\%$.) Narath's data at 4 °K are from a direct measurement of M (Ref. 1).

(ii) Demagnetizing effects, depending only on geometry, would not be expected to be strongly temperature dependent, but a sharp temperature dependence of the hysteresis is observed.

Recently, Tinkham²⁷ has theoretically described in detail the dynamics of the microscopic spin reorientations which occur at H_{C1} and H_{C2} in near-Ising $\text{CoCl}_2 \cdot 2\text{H}_2\text{O}$. Although FC2 is not a near-Ising spin system, we might expect similar qualitative behavior for its metamagnetic transitions. Tinkham has shown that the nucleation rate for the transition at H_{C2} is far faster than that at H_{C1} . It is predicted that no hysteresis should be observed at H_{C2} . The transition we observe at H_{C1} , however, is much more complicated and probably dominated by nucleation at defect sites; hysteresis at H_{C1} is not ruled out, nor is it unexpected. If there were hysteresis with this origin, it would be predicted to be less at higher temperatures, as we observe. Tinkham's approach thus accounts for many general features of the observed hysteresis, although certainly many other features remain unexplained. For example, it is not understood why, upon decreasing the field from H_{C2} , the AF domains are nucleated *above* H_{C1} .

VI. DISCUSSION

Measurement of the far-infrared absorption spectrum of $\text{FeCl}_2 \cdot 2\text{H}_2\text{O}$ (FC2) in all three metamagnetic phases has enabled us to determine *both* the magnitude and the anisotropy of the exchange interactions J_1 and J_2 : We show that these interactions are isotropic. The measured g value $g_{\parallel} = 2.23$, together with the saturation magnetization measurement ($g_{\parallel} S \approx 4.25$), enable us to establish

that the effective spin of the ground state is $S = 2$, the free ion value. This is in agreement with the results of Johnson's Mössbauer work.² Since the simple Curie-Weiss expression⁷ for the paramagnetic susceptibility is only approximately correct for $kT \sim D$, measurements of both $\chi_{||}$ and $g_{||}S$ do not uniquely determine the value of S . Inomata and Oguchi³ used $\chi_{||}$ and $g_{||}S$ to obtain $S = 1$, which is inconsistent with experiment.

Our microscopic measurements of $g_{||} = 2.23 \pm 0.02$, $H_{C1} = 35.0 \pm 0.5$ kOe, and $H_{C2} = 45.0 \pm 0.5$ kOe are to be compared to Narath's macroscopic determination of $g_{||} = 2.4$ (and 2.13 ± 0.03 , from $g_{||}S = 4.25$), $H_{C1} = 39.2$ kOe, and $H_{C2} = 45.6$ kOe. It should be noted that our values of H_{C1} and H_{C2} were obtained from analysis of the spin-wave energies using the theoretical relations (12) and (13), rather than from a direct measurement of the transition fields. The agreement between the theoretical parameters " H_{C1} " and " H_{C2} " and the transition fields provides verification of (12) and (13). Note that the parameter " H_{C1} " (35.0 kOe) appears at the onset of the Fi absorption (Fig. 6), rather than at the midpoint of the transition. Using the latter criterion, we would find a value of $H_{C1} \sim 37$ kOe at 4 °K, which compares more favorably with Narath's value 39.2 kOe. (Note that Narath's somewhat higher values of H_{C1} and H_{C2} and lower value of $g_{||}S$ may, in part, be caused by sample or alignment problems.)

It is interesting to compare the results of FC2 with the results obtained in isomorphous $\text{CoCl}_2 \cdot 2\text{H}_2\text{O}$ (CC2),^{4,10} which has approximately the same values of T_N , H_{C1} , and H_{C2} .²⁸ The mean spin wave

and phonon energies are also very similar. In CC2, however, the longitudinal anisotropy is much larger than in FC2 and (at these temperatures and energies) it is convenient to make a transformation to a fictitious spin $S = \frac{1}{2}$. (The ionic spin of Co^{2+} is $\frac{3}{2}$). In terms of this effective spin, the exchange interactions (assumed isotropic) are transformed into *anisotropic* effective exchange interactions, which contain the magnetic anisotropy. In FC2, it is not convenient to make such a transformation; the exchange interactions remain isotropic and the magnetic anisotropy is contained in the D term. These differences between Co^{2+} and Fe^{2+} give rise to (minor) differences in the observed spin-wave spectra, which are well accounted for by theory. More dramatic differences, however, are expected in the higher-lying levels. Bound states of more than one magnon, for example, have been predicted to exist²⁹ and, in fact, have been directly observed for the first time in CC2.⁴ The energies of these states depend strongly on the spin and longitudinal anisotropy. The differences between Fe^{2+} and Co^{2+} in these materials should give rise to markedly different magnon bound-state spectra.^{4,30} These predictions could not have been confirmed, however, because bound states have not been observed in FC2. This is as expected, since the nearly uniaxial symmetry in FC2 implies that the absorption coefficient for exciting bound states is small.⁴

ACKNOWLEDGMENT

It is a pleasure to thank M. Tinkham for valuable discussions.

[†]Work partially supported by the National Science Foundation, Advanced Research Projects Agency and the Office of Naval Research.

*NATO Postdoctoral Fellow. Present address: Central Electricity Research Laboratories, Materials Division, Leatherhead, England.

[‡]Present address: IBM Thomas J. Watson Research Center, P.O. Box 218, Yorktown Heights, N.Y. 10598.

¹A. Narath, Phys. Rev. **139**, A1221 (1965); A. Narath and J. E. Schirber, J. Appl. Phys. **37**, 1124 (1966).

²C. E. Johnson, Proc. Phys. Soc. (London) **88**, 943 (1966).

³K. Inomata and T. Oguchi, J. Phys. Soc. Japan **23**, 765 (1967); **28**, 905 (1970).

⁴J. B. Torrance, Jr., and M. Tinkham, J. Appl. Phys. **39**, 822 (1968); Phys. Rev. **187**, 595 (1969); **187**, 587 (1969).

⁵K. A. Hay and J. B. Torrance, Jr., J. Appl. Phys. **40**, 999 (1969).

⁶B. Morosin and E. J. Graeber, J. Chem. Phys. **42**, 898 (1965).

⁷ $\chi_i = N g_i^2 \mu_B^2 S(S+1)/3k(T - \Delta_i)$, $i = \alpha, \beta, \gamma$.

⁸This method was suggested by M. Tinkham.

⁹A. H. Morrish, *The Physical Principles of Magnetism* (Wiley, New York, 1965).

¹⁰J. B. Torrance, Jr., Ph.D. thesis, Harvard University, 1968 (unpublished); Harvard University Technical Report No. 1, D.E.A.P., 1969 (unpublished).

¹¹This system, designed and constructed by R. S. Newbower and P. C. L. Tai, is briefly described in Ref. 10.

¹²S. Roberts, General Electric Report No. 67-C-303, 1967 (unpublished).

¹³Westinghouse superconducting solenoid, 1½-in. bore, 55-kOe max field with 1% homogeneity over the sample volume. Calibrated by J. Gollub.

¹⁴Buckbee-Mears Co., St. Paul, Minn.

¹⁵I. F. Silvera, Ph.D. thesis, University of California, Berkeley, 1965 (unpublished).

¹⁶S. J. Allen and H. J. Guggenheim, Phys. Rev. Letters **21**, 1807 (1968).

¹⁷C. Kittel, *Quantum Theory of Solids* (Wiley, New

York, 1963), Chap. 4; F. Keffer, in *Handbuch der Physik* (Springer-Verlag, Berlin, 1966), Vol. XVIII/2.

¹⁸A. Narath, *Phys. Letters* **13**, 12 (1964).

¹⁹M. Tinkham, *Phys. Rev.* **124**, 311 (1961).

²⁰I. F. Silvera, J. H. M. Thornley, and M. Tinkham, *Phys. Rev.* **136**, A695 (1964).

²¹A. Abragam and M. H. L. Pryce, *Proc. Roy. Soc. (London)* **A205**, 135 (1951); C. J. Ballhausen, *Introduction to Ligand Field Theory* (McGraw-Hill, New York, 1962).

²²A. A. Missetich and T. Buch, *J. Chem. Phys.* **41**, 2524 (1964); A. A. Missetich and R. E. Watson, *Phys. Rev.* **143**, 355 (1966).

²³R. C. Ohlmann and M. Tinkham, *Phys. Rev.* **123**,

425 (1961).

²⁴M. Tinkham, *Proc. Roy. Soc. (London)* **A236**, 535 (1956).

²⁵J. B. Torrance, Jr., and K. A. Hay (unpublished); Ref. 10.

²⁶I. S. Jacobs, S. Roberts, and P. E. Lawrence, *J. Appl. Phys.* **36**, 1197 (1965).

²⁷M. Tinkham, *Phys. Rev.* **188**, 967 (1969).

²⁸A. Narath, *Phys. Rev.* **136**, A766 (1964).

²⁹H. A. Bethe, *Z. Physik* **71**, 205 (1931); M. Wortis, *Phys. Rev.* **132**, 85 (1963); J. Hanus, *Phys. Rev. Letters* **11**, 336 (1963).

³⁰R. Silbergliitt and J. B. Torrance, Jr., *Phys. Rev.* (to be published).

PHYSICAL REVIEW B

VOLUME 2, NUMBER 3

1 AUGUST 1970

Possible Species of Ferromagnetic, Ferroelectric, and Ferroelastic Crystals

Kêitsiro Aizu

Hitachi Central Research Laboratory, Kokubunzi, Tokyo, Japan

(Received 17 November 1969)

A ferromagnetic, ferroelectric, or ferroelastic crystal is called full or partial, according to whether all or not all but some of its orientation states are different in spontaneous magnetization vector, spontaneous polarization vector, or spontaneous strain tensor. In previous theories—for nonmagnetic crystals—the concept of “species” was introduced, a determination was made of all possible species of full ferroelectrics and of full ferroelastics, and those species were found in which ferroelectricity and ferroelasticity coexist and completely couple with each other. These theories are now extended to cover magnetic crystals in addition to nonmagnetic crystals and to cover the partial in addition to the full. A determination is made of all possible species of full ferromagnetics, partial ferromagnetics, full ferroelectrics, partial ferroelectrics, full ferroelastics, and partial ferroelastics, and it is found out in which of these species two or all of ferromagnetism, ferroelectricity, and ferroelasticity should couple completely or incompletely with each other.

1. INTRODUCTION

A crystal is provisionally referred to as being “ferroic” when it has two or more orientation states in the absence of magnetic field, electric field, and mechanical stress and can shift from one to another of these states by means of a magnetic field, an electric field, a mechanical stress, or a combination of these. Here any two of the orientation states are identical or enantiomorphous in structure but are different with respect to direction of arrangement of atoms which may possess an electric charge, an electric dipole moment, and a magnetic dipole moment.

The ferromagnetic crystals are those ferroic crystals whose orientation states are all different in spontaneous magnetization vector. The ferroelectric crystals are those ferroic crystals whose

orientation states are all different in spontaneous polarization vector. There are ferro crystals whose orientation states are all different in spontaneous strain tensor. (In this paper, “spontaneous strain tensor” means simply “strain tensor at null stress.”) They are called ferroelastic.¹ In the ferromagnetic crystals the shift between any two orientation states can be brought about by a magnetic field; in the ferroelectric crystals the shift between any two orientation states can be brought about by an electric field, and in the ferroelastic crystals, by a mechanical stress.

Precisely speaking, the above-defined ferromagnetics, ferroelectrics, and ferroelastics are *full* ferromagnetics, full ferroelectrics, and full ferroelastics, respectively. Ferroics are possible, not all but some of whose orientation states are different in spontaneous magnetization vector,